NANOFABRICATION OF SPLIT RING RESONATOR STRUCTURES FOR NEGATIVE REFRACTIVE INDEX MATERIALS IN OPTICAL RANGE

Zoran Jakšić, Dana Vasiljević-Radović, Milan Maksimović, Milija Sarajlić
IHTM – Institute of Microelectronic Technologies and Single Crystals, Njegoševa 12, 11000 Beograd

Abstract – *We performed experimental nanofabrication of planar split-ring resonator structures for one-dimensional metamaterials with negative refractive index in mid- and long-wavelength infrared range. We fabricated double split ring and complementary double split ring resonators (SRR and CSRR) with square and circular geometries. We used scanning probe nanolithography with z-scanner movement to fabricate straight-line and curvilinear segments with a line width of 60-80 nm. The geometries were delineated in 20 nm thin silver layers sputter-deposited on positive photoresist substrate spin-coated on polished single crystal silicon wafers. The morphology of the structures was characterized by the atomic force microscope.*

1. INTRODUCTION

Electromagnetic metamaterials with negative refractive index (NRI) [1], [2] may be defined as artificial subwavelength structures designed to simultaneously reach negative values of effective dielectric permittivity (ε) and magnetic permeability (μ) in a given wavelength range, thus having a negative value of effective refractive index. According to the *Science* magazine, NRI materials were among the top ten scientific breakthroughs of the year 2003 [3].

The direction of the Pointing vector in a negative index metamaterial is opposite to that of the wavevector, i.e. the vectors of the electric and magnetic field and the wavevector form a left-oriented set. NRI materials are thus sometimes called left-handed metamaterials. Among other names used for this specific type of artificial materials are double negative materials, backward media and Veselago media.

NRI materials were first theoretically described by Viktor Veselago [4]. Independently of Veselago's works, Pendry rediscovered the same effect and proposed methods for its practical implementation [5], [6], [7]. The first experimental NRI materials were realized in experiments of Smith et al [8].

There are many different phenomena peculiar for NRI materials – reversal of Snell's law the Doppler shift and the Cerenkov effect [1]. A number of novel applications were proposed using NRI. Probably the most important among them are "superlenses" or "perfect lenses" [9] which focus all Fourier components of a 2D image, including evanescent modes, thus furnishing resolutions beyond the diffraction limit. Another proposed application is subwavelength resonant structure [10], i.e. a resonator with its dimensions much smaller than the operating wavelength.

Different practical solutions stemmed from these, e.g. high-gain, electrically small antennas for the microwave, materials possessing magnetic properties at THz frequencies, different microwave transmission lines [10], directional couplers, resonators, filters, antireflection structures, but also active optical elements based on nonlinear phenomena, etc. [11].

The first experimental building blocks acting as NRI metamaterials included thin metallic wires [4] with negative effective dielectric permittivity, and split ring resonators (SRR) for negative magnetic permeability [5]. The SRR (negative permeability elements, also described in literature as 'particles' or 'meta-atoms' of NRI [1]) are arranged in unit cells whose multiplication furnishes macroscopic NRI medium. Even though alternative methods were proposed for the fabrication of NRI materials using transmission line approach [12], the SRR remains one of the basic building blocks used to achieve $\mu<0$.

Different versions of single and double split rings were analyzed in a number of papers, their operating wavelengths ranging from the microwave to the infrared. Some of the proposed geometries are described in 2005 article [13].

In November 2004 Phys. Rev. Lett. [14] a complementary split ring resonator structure was proposed. Such structures furnish a negative dielectric permittivity and thus are the first 'particle' alternative to thin wire and transmission line structures.

Since the NRI material building block dimensions have to be strongly subwavelength, it is a difficult technological task to fabricate such structures for the optical range. The smallest experimental SRRs features produced so far had features of about 5 μm, rendering a response in infrared [1]. Some theoretical solutions to reach the near infrared wavelengths, and specifically 1.55 μm operating wavelength were described in [15].

In this paper we analyze a possibility to fabricate planar NRI metamaterials ('metasurfaces') for the optical wavelength range using scanning probe nanolithography. We analyzed different planar designs utilizing the ordinary and complementary split ring structures and performed experiments on their fabrication on our scanning probe nanolithographic system. The fabricated samples were characterized by the atomic force microscopy (AFM).

2. THEORY

The basic building block of NRI materials, the double split ring resonator (SRR) is a highly conductive ($\sigma\rightarrow\infty$) structure in which the capacitance between its two rings is large and balances its inductance. A time-varying magnetic field applied perpendicular to the rings surface induces currents which, in dependence on the resonant properties of the structure, produce a magnetic field that may either oppose or enhance the incident field, thus resulting in positive or negative effective permeability. Complementary split ring (CSRR) is a "negative" geometry to that of an SRR and according to the Babinet principle it is the unit cell of metamaterial/metasurfaces furnishing negative ε [14].

Fig. 1 shows the square and circular geometries we chose to consider for our design. The top left drawing shows the original SRR geometry with one capacitive gap per ring,

while the bottom row shows our geometries with several capacitive gaps. Circular geometries are shown in the top row, and linear in the bottom row. The right column shows the complementary structures.

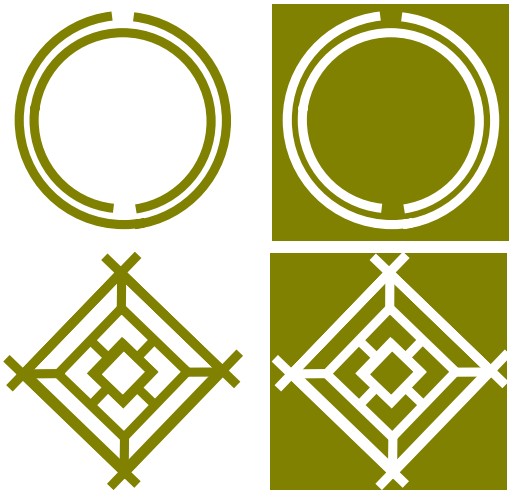

Fig. 1. *Some double split ring geometries convenient for the optical range (shaded areas denote metal surface, white are nanolithographic 'cuts'). Top and bottom left: ordinary SRR; top and bottom right: complementary SRR. Top row utilizes circular and bottom row linear line segments.*

The effective permeability and permittivity across a NRI material unit cell are obtained as

$$\left(\mu_{eff}\right)_{x_i} = \frac{\langle B \rangle_{x_i}}{\mu_0 \langle H \rangle_{x_i}}, \quad \left(\varepsilon_{eff}\right)_{x_i} = \frac{\langle D \rangle_{x_i}}{\varepsilon_0 \langle E \rangle_{x_i}} . \tag{1}$$

For the split ring resonator shown in Fig. 1 top left for the case when the rings are in vacuum and their thickness is neglected the following approximate expression is valid [7]

$$\mu_{eff} = 1 - \frac{\pi r^2 / s}{1 + \frac{2\sigma i}{\omega \tau \mu_0} - \frac{3d}{\pi^2 \mu_0 \omega^2 \varepsilon_0 r^3}} , \tag{2}$$

where r is the unit cell length, d is the gap between the rings, and σ is electrical conductance.

The resonant frequency (for which $\mu_{eff} \to \pm\infty$)

$$\omega_{0m} = \sqrt{\frac{3dc_0^2}{\pi^2 r^3}} , \tag{3}$$

while the magnetic plasma frequency (for which $\mu_{eff} \to 0$)

$$\omega_{pm} = \sqrt{\frac{3dc_0^2}{\pi^2 r^3 \left(1 - \pi r^2 / a^2\right)}} . \tag{4}$$

For a dielectric with ε and a ring line width w [15]

$$\omega_{0m} = \sqrt{\frac{3dc_0^2}{\pi \varepsilon r^3 \ln(2w/d)}} . \tag{5}$$

Based on (2)-(5) the necessary unit cell dimensions to reach the optical wavelength range are readily calculated. For a circular split ring structure we chose a ratio of the unit cell to the SRR radius of 0.4. We calculated the structure response for different inter-ring spacing values d. The unit cell dimensions must be 5-10 times smaller than the operating wavelength, depending on the chosen gap within the SRR. If nanolithographic lines of the order of 0.1 μm are used (which defines the minimum gap between rings), structures with minimum features 1.5-4 μm can be designed, thus the target wavelengths would be about 5-10 μm (mid- to long-wavelength infrared).

Another issue to be considered is the high frequency scalability of the forms described by eqs. (2)-(4). The thickness of the metal layers for the SRR/CSRR must not be smaller than the skin depth [15] (approx. 20 nm for silver at 100 THz). Additionally, at wavelengths approaching the optical range there is an additional inductance determining the plasma frequency, termed inertial inductance, which is a consequence of the electron mass and the currents through the SRR being almost purely ballistic [1]. Thus for the scaled-down dimensions the inertial inductance becomes prevailing and the negative permeability/permittivity effect completely disappears. A method to overcome this problem was proposed in [15]. To this purpose more capacitive gaps are added to the original SRR design.

The bottom row of Fig. 1 (linear segments) shows double SRR and CSRR structures where additional capacitive gaps have been introduced to compensate for inertial inductance. The geometries shown in the top row can be modified in the same manner.

The geometries shown in the bottom row represent our modification of the recently proposed ones ([13] and [15]) done with the aim to further decrease the undesirable effects of inertial inductance.

3. NANOFABRICATION

We started our sample preparation by using double polished silicon wafers. The wafers were spin-coated by positive photoresist, 400 nm thickness and dried without baking. Further we used rf sputtering to deposit a 20 nm thick silver layer over the photoresist. The surface morphology prior to nanolithography was characterized by atomic force microscopy. The flatness of the silver surface was better than 2 nm.

Thus prepared surfaces were nanolithographically processed to obtain NRI material building blocks. To this purpose we utilized scanning probe nanolithography on our Veeco Autoprobe CP-Research atomic force microscope (AFM).

The nanolithography process was done under operating conditions standard for microelectronics/MEMS. That means that it was performed under normal atmospheric pressure and at room temperature and humidity. However, antivibration and shock-free conditions were absolutely essential for proper operation. Such conditions were ensured by an anti-vibration table unit with active oscillation dumping. It is worth mentioning that even this sometimes failed to ensure disturbance-free operation.

There are three modes of operation available on the Autoprobe CP-Research AFM: z-scanner movement ('scratching' mode), the voltage pulse mode (direct forming of oxide on the surface of silicon or other semiconductors) and the set-point nanolithography (the constant load mode). Of these three we chose the z-scanner movement mode.

A silicon nitride microcantilever tip was used for the operation. The scanner base position was adjusted to between 0.7 μm and 0.9 μm below the zero position, thus effectively pressing needle tip against the sample surface with different forces of the order of nN. The real depth and width of the obtained nanolithographic lines depended on that force, on the needle tip shape, sample surface material and the needle tip speed (the slower the speed, the larger the depth).

4. EXPERIMENTAL RESULTS

Fig. 2 shows the profiles of nanolithographic lines formed in silver layers on photoresist substrate.

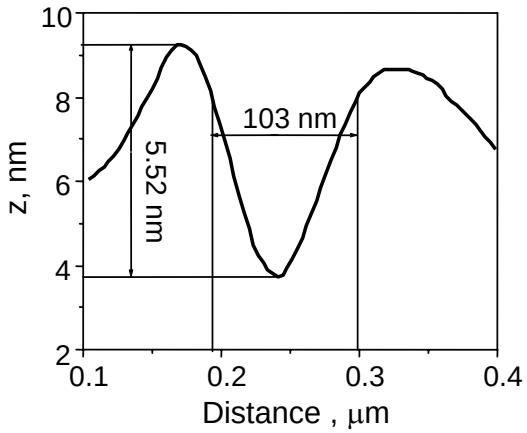

Fig. 2. *Profiles and dimensions of different nanolithographic lines fabricated in silver on photoresist.*

It can be seen that the z-scanner movement nanolithography actually digs a groove in the substrate and leaves the 'upturned' material on its edges. This does not represent a problem with our structures of choice, since it is only important to physically disconnect thin metal surfaces while retaining the geometries as shown in Fig. 1.

Fig. 3 shows our fabricated straight-line (square) segment-based SRR structure. Each ring is split into four segments and the whole structure diagonal is 2.5 μm, while its inner square diagonal is about 1 μm. The z-scanner displacement was -0.7 μm and the nanolithographic line width was about 60 nm. Some lines in the obtained structure were displaced 60-150 nm compared to the designed ones. Repeatability was tested by nanofabricating several identical structures and it also ranged between 60 and 150 nm.

Fig. 4 (top and bottom) shows two complementary split ring structures with curvilinear segments, differing in the widths of their capacitive gaps. The outer diameter of the CSRRs was 2.2 μm, while the inner ring diameter was about 1 μm. The z-displacement here was larger (–0.9 μm), resulting in wider nanolithographic lines (about 80 nm).

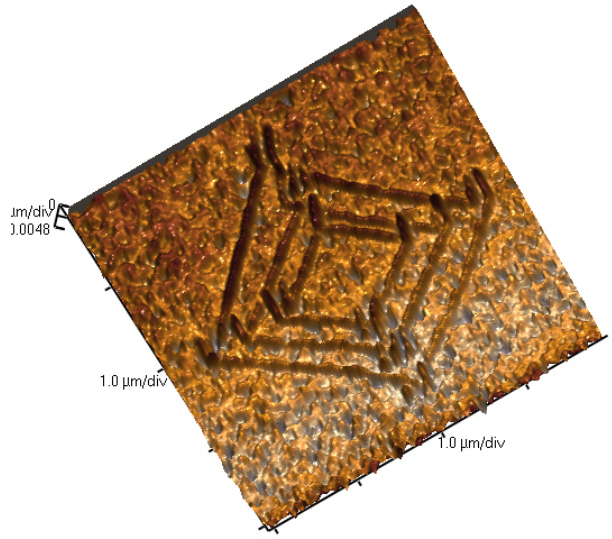

Fig. 3. *AFM profile of our square double split ring resonator structure fabricated by SPM nanolithography.*

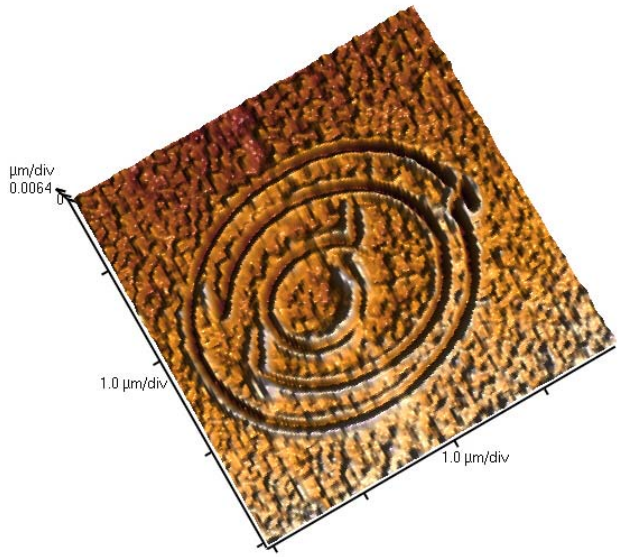

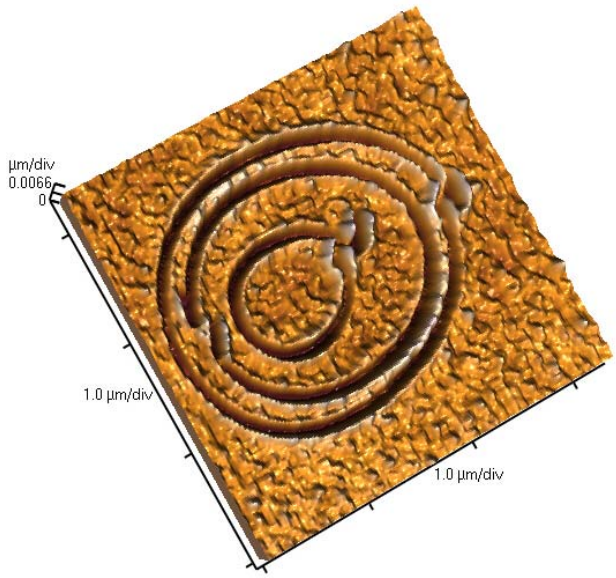

Fig. 4. *AFM profiles of two different double CSRR structures fabricated by SPM nanolithography.*

The process duration for a single SRR or CSRR took several seconds for straight-line segments, but it lasted 2-3 minutes for each curvilinear feature. The reason is that a circle is actually drawn as up to 360 linear segments. Additionally, each nanolithographic pattern requires full surface scanning before and after the process. Thus the fabrication of more complex patterns containing a larger number of elements ('particles') could be painstakingly slow.

Among the largest problems noted with the nanofabrication of the SRR and CSRR geometries were gradual 'shifting' of the fabricated patterns compared to the designed ones, most noticeable in slight curving of otherwise straight segments or in designed circles becoming spirals. An additional problem was that in some patterns a 'kink' at the beginning and at the end of each line appeared, 100 nm to 300 nm long, probably caused by the operation of the piezo-actuated micropositioner.

An advantageous property of the chosen silver substrates was that these were readily formed by the gallium nitride needle tip.

5. CONCLUSION

The basic double split ring and complementary double split ring resonator (SRR and CSRR) geometries for the NRI materials in optical wavelength range have been fabricated using z-scanner movement nanolithography in 20 nm thick silver layers. We characterized the obtained morphology of our samples by AFM. The best achieved resolution was 60-80 nm, and the feature repeatability was 60-150 nm, depending on the process conditions and the feature complexity. The nanolithographic groove depth in different samples ranged from 4 nm to 80 nm.

Our further works should include fabrication of other alternative geometries and the production of larger 2D arrays of negative μ and ε particles, as well as the electromagnetic characterization of thus obtained metasurfaces. This should include spectral transmission measurements by IR microscopy as well as magnetic force microscopy measurements of metasurfaces.

ACKNOWLEDGMENT

The authors wish to thank Ms. Mirjana Popović, BSCE and Ms. Kristina Blagojević, IHTM-IMTM for their preparation of sample substrates. This work was partially funded by the Serbian Ministry of Science and Environmental Protection within the framework of the Project TR-6151B.

REFERENCES

[1] S. A. Ramakrishna, "Physics of negative refractive index materials", *Rep. Prog. Phys*. **68**, pp. 449–521, 2005

[2] J. B. Pendry, D. R. Smith, "Reversing Light: Negative Refraction", *Physics Today*, **57**, pp. 37-44, 2004.

[3] "Breakthrough of the year: The runners-up," *Science*, 302, 5653, pp. 2039–2045, 2003.

[4] V.G. Veselago, "The electrodynamics of substances with simultaneously negative values of ε and μ", *Sov. Phys. Uspekhi*, **10**, pp. 509-514, 1968.

[5] J. B. Pendry, A. J. Holden and W. J. Stewart, I. Youngs, "Extremely Low Frequency Plasmons in Metallic Mesostructures", *Phys. Rev. Lett.*, **76**, pp. 4773-4776, 1996.

[6] J. B. Pendry, A J Holdenz, D. J. Robbinsz and W. J. Stewartz, "Low Frequency Plasmons in Thin Wire Structures", *J. Phys.: Condens. Matter* **10**, pp. 4785-4788, 1998.

[7] J. B. Pendry, A. J. Holden, D. J. Robbins, and W. J. Stewart, "Magnetism from conductors and enhanced nonlinear phenomena", *IEEE Trans. on Microwave Theory and Tech*., **47** pp. 2075-2084, 1999

[8] D. R. Smith, W. J. Padilla, D. C. Vier, D. C. Nemal-Nasser, S. Schultz, "Composite medium with simultaneously negative permeability and permittivity", *Phys. Rev. Lett*., **84**, pp. 4184-4187, 2000.

[9] J. B. Pendry, "Negative Refraction Makes a Perfect Lens", *Phys. Rev. Lett*., **85**, pp. 3966-3969, 2000.

[10] N. Engheta, "An Idea for Thin Subwavelength Cavity Resonators Using Metamaterials With Negative Permittivity and Permeability", *IEEE Ant. Wireless Propag. Lett*, Vol. **1**, No. 1, pp. 10-13, 2002.

[11] A. Lai, C. Caloz, T. Itoh, "Composite Right/Left-Handed Transmission Line Metamaterials", *IEEE Microwave Magaz*. pp. 34-50, 2004.

[12] G. V. Eleftheriades, A. K. Iyer, "Planar Negative Refractive Index Media Using Periodically *L–C* Loaded Transmission Lines", *IEEE Trans. Microw. Theory Techniques*, **50**, 12, pp. 2702-2712, 2002.

[13] M. Kafesaki, Th. Koschny, R. S. Penciu, T. F. Gundogdu, E. N. Economou, C. M. Soukoulis, " Left-handed metamaterials: detailed numerical studies of the transmission properties", *J. Opt. A: Pure Appl. Opt*., **7** pp. S12–S22, 2005

[14] F. Falcone, T. Lopetegi, M. A. G. Laso, J. D. Baena, J. Bonache, M. Beruete, R. Marques, F. Martin, M. Sorolla, "Babinet Principle Applied to the Design of Metasurfaces and Metamaterials", *Phys. Rev. Lett*. **93**, 19, pp. 197401-1-4, Nov. 2004.

[15] S. O'Brien, D. McPeake, S. A. Ramakrishna, J. B. Pendry, "Near-Infrared Photonic Band Gaps and Nonlinear effects in Negative Magnetic Metamaterials", *Phys. Rev. B*. **69**, pp. 241101-1-4, 2004.

[16] F. J. Rachford, D. L. Smith, P. F. Loschialpo, D. W. Forester, "Calculations and measurements of wire and/or split-ring negative index media", *Phys. Rev. E*, **66**, pp. 036613-1-4, 2002.